BULETINUL INSTITUTULUI POLITEHNIC DIN IAŞI
Publicat de
Universitatea Tehnică „Gheorghe Asachi” din Iaşi
Volumul 64 (68), Numărul 3, 2018
Secția
ELECTROTEHNICĂ. ENERGETICĂ. ELECTRONICĂ

ONLINE COMPENSATION OF EFFECTS CAUSED OF THE INDUCTION MOTOR ELECTRICAL PARAMETERS VARIATIONS FOR EXTENDED LUENBERGER OBSERVER

BY

OLIMPIU STOICUȚA[1,*], TEODOR PANĂ[2], ROBIN MOLNAR[2], EMIL SERGIU ANDRAŞ[2] and DANIEL DEACONU[2]

[1]University of Petroşani
Departament of Control Engineering, Computer, Electrical Engineering and Power Engineering
[2]Technical University of Cluj-Napoca
Departament of Electrical Machines and Drives

Received: September 3, 2018
Accepted for publication: October 10, 2018

Abstract. The article presents a solution to compensate for the effects caused of the induction motor electric parameters variations for extended Luenberger observer (ELO), used in the simultaneous estimation of the rotor speed, position and module of the rotor flux phasor. ELO is adjusted according to the estimated stator and rotor time constants. The rotor time constant is estimated based on a relationship deducted from the mathematical model of the induction motor. The dynamic performances of the extended Luenberger observer are highlighted by simulation, in Matlab-Simulink.

Key words: extended Luenberger observer; speed estimation; rotor resistance estimation; sensorless vector control system; induction motors.

1. Introduction

The simultaneous estimation of the speed and rotor resistance of the induction motor, in the sensorless vector control systems, is an unresolved issue that raises problems in implementing control system. In this regard we recall here the results of the research of (Kubota *et al.*, 1993; Kubota *et al.*, 1994) and

[*]Corresponding author: *e-mail*: OlimpiuStoicuta@upet.ro

(Shinnaka, 1993). In the research of (Kubota *et al*., 1994, p. 1222) it is shown that, in the vector control systems, in the stationary regime, only the proportionality relation between slip angular frequency and rotor resistance (ω_s/Rr) can be estimated, because it is impossible to separate from the stator state variables, error estimation of the speed of the estimation of the rotor resistance. In other words, in stationary regime the condition of persistence of excitation is not respected. On the other hand, (Shinnaka, 1993) demonstrates that estimating both the speed and the rotor resistance implies a division with zero if the module of the rotor flux phasor is maintained constant.

In view of the above, the paper presents a method of simultaneous estimation of the speed, rotor resistance and stator resistance of an induction motor, from the sensorless vector control system. Within the vector control system, speed and rotor flux of the induction motor are estimated by the extended Luenberger observer and rotor resistance is estimated using a relationship obtained from the mathematical model of the induction motor. Stator resistance is estimated based on an adaptive scheme.

In order to eliminate the issue of persistence of excitation, a sinusoidal signal of frequency and amplitude low is used, which is superimposed over the module of the phasor rotor flux reference (Kubota *et al*., 1994, p. 1223), and to avoid zero division is used "Fixed Trace" method proposed by (Pana *et al*., 1995; Pană, 1996). The dynamic performances of the extended Luenberger observer compensated by the rotor resistance and stator resistance, are analyzed by simulation using the Matlab-Simulink program.

2. The Extended Luenberger Observer

The equations that define this observer are shown in the following relations (Kubota *et al*., 1994, p. 1220)

$$\frac{\mathrm{d}}{\mathrm{d}t}\begin{bmatrix}\hat{\underline{i}}_s(t)\\ \hat{\underline{\psi}}_r(t)\end{bmatrix}=\begin{bmatrix}a_{11}^* & a_{12}^*(t)\\ a_{21}^* & a_{22}^*(t)\end{bmatrix}\cdot\begin{bmatrix}\hat{\underline{i}}_s(t)\\ \hat{\underline{\psi}}_r(t)\end{bmatrix}+\begin{bmatrix}b_{11}^*\\ 0\end{bmatrix}\cdot\underline{u}_s+L(t)\cdot\left[\underline{i}_s(t)-\hat{\underline{i}}_s(t)\right]; \quad (1)$$

$$\hat{\omega}_r(t)=K_{Ra}f(t)+K_{Ia}\int_0^t f(\tau)\,d\tau\,, \quad (2)$$

where:

$$\hat{\underline{\psi}}_r(t)=\hat{\psi}_{dr}(t)+j\hat{\psi}_{qr}(t);\ j=\sqrt{-1};$$

$$f(t)=e_a(t)\hat{\psi}_{qr}(t)-e_b(t)\hat{\psi}_{dr}(t);\ e_a(t)=i_{ds}(t)-\hat{i}_{ds}(t);\ e_b(t)=i_{qs}(t)-\hat{i}_{qs}(t);$$

$$\hat{\underline{i}}_s(t)=\hat{i}_{ds}(t)+j\hat{i}_{qs}(t);\ \underline{i}_s(t)=i_{ds}(t)+ji_{qs}(t);\ \underline{u}_s(t)=u_{ds}(t)+ju_{qs}(t);$$

$$a_{11}^*=-\left(\frac{1}{T_s^*\sigma^*}+\frac{1-\sigma^*}{T_r^*\sigma^*}\right);\ a_{12}^*(t)=a_{13}^*-ja_{14}^*z_p\hat{\omega}_r(t);\ a_{21}^*=a_{31}^*;$$

$$a_{22}^*(t)=a_{33}^*+jz_p\hat{\omega}_r(t);\ a_{13}^*=\frac{L_m^*}{L_s^*L_r^*T_r^*\sigma^*};\ a_{14}^*=\frac{L_m^*}{L_s^*L_r^*\sigma^*};\ a_{31}^*=\frac{L_m^*}{T_r^*};\ a_{33}^*=-\frac{1}{T_r^*};$$

$$b_{11}^*=\frac{1}{L_s^*\sigma^*};\ \sigma^*=1-\frac{\left(L_m^*\right)^2}{L_s^*L_r^*};\ T_s^*=\frac{L_s^*}{R_s^*};\ T_r^*=\frac{L_r^*}{R_r^*}.$$

The Luenberger matrix what is obtained from the proportionality condition between the motor's eigenvalues and the Luenberger observer's eigenvalues, is

$$L(t)=\begin{bmatrix}L_{11}+jL_{12}(t)\\ L_{21}+jL_{22}(t)\end{bmatrix} \tag{3}$$

where:

$$L_{11}=(1-k)\left(a_{11}^*+a_{33}^*\right);\ L_{12}(t)=(1-k)z_p\hat{\omega}_r(t);$$

$$L_{21}=\left(a_{31}^*+\frac{a_{11}^*}{a_{14}^*}\right)\left(1-k^2\right)-\frac{1}{a_{14}^*}L_{11};\ L_{22}(t)=-\frac{1}{a_{14}^*}L_{12}(t).$$

The block diagram of the extended Luenberger observer (ELO) is presented in Fig. 1.

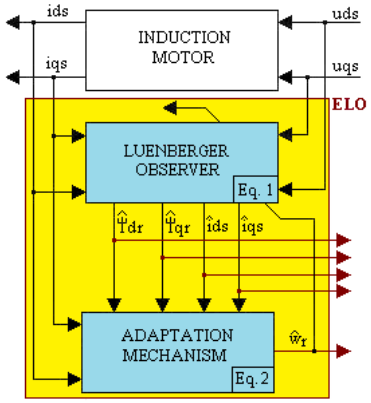

Fig. 1 − The Extended Luenberger Observer (ELO).

In the above relations, K_{Ra} and K_{Ia} constants are chosen to obtain the desired dynamic regime.

The proportionality coefficient between the motor's eigenvalues and the Luenberger observer's eigenvalues, is noted „*k*". From the above relationships, we can see that the coefficients a_{12}^* and a_{22}^*, as well as the coefficients L_{12} and

L_{22}, adapt to each moment of time according to the estimated speed. In the above relations, we marked with „*", the electrical parameters of the induction motor off-line identify (DC test or AC test), and by „^" the electrical variables estimated on-line.

3. The ELO Adaptation According to Stator and Rotor Time Constants

The stator time constant is estimated using the following relationship (Kubota *et al.*, 1993, p. 1223)

$$\frac{1}{\hat{T}_s(t)} = -\left[K_{Rb} g(t) + K_{Ib} \int_0^t g(\tau)\,\mathrm{d}\tau \right], \tag{4}$$

where: $g(t) = e_a(t)\hat{i}_{ds}(t) + e_b(t)\hat{i}_{qs}(t)$, $e_a = i_{ds} - \hat{i}_{ds}$, $e_b = i_{qs} - \hat{i}_{qs}$, and K_{Rb}, K_{Ib} constants are chosen to obtain the desired dynamic regime.

To determine the mathematical expression that is used in the estimation of rotor resistance, we will present below, the voltage equations specific to the squirrel-cage rotor of an induction motor (Pană, 2016):

$$\begin{cases} \dfrac{\mathrm{d}}{\mathrm{d}t}\psi_{dr} = -R_r i_{dr} - z_p \omega_r \psi_{qr}, \\ \dfrac{\mathrm{d}}{\mathrm{d}t}\psi_{qr} = -R_r i_{qr} + z_p \omega_r \psi_{dr}. \end{cases} \tag{5}$$

After solving the above system, the rotor speed is given by the following expression:

$$R_r = -\frac{\psi_{dr}\dfrac{\mathrm{d}}{\mathrm{d}t}\psi_{dr} + \psi_{qr}\dfrac{\mathrm{d}}{\mathrm{d}t}\psi_{qr}}{\psi_{dr} i_{dr} + \psi_{qr} i_{qr}}. \tag{6}$$

On the other hand, the rotor flux equations of the induction motor are:

$$\begin{cases} \psi_{dr} = L_r i_{dr} + L_m i_{ds}, \\ \psi_{qr} = L_r i_{qr} + L_m i_{qs}. \end{cases} \tag{7}$$

From (7), the rotor currents are:

$$i_{dr} = \frac{1}{L_r}\left(\psi_{dr} - L_m i_{ds}\right); i_{qr} = \frac{1}{L_r}\left(\psi_{qr} - L_m i_{qs}\right). \tag{8}$$

After the introduction of relations (8) into (6), we get the following:

$$R_r = -L_r \frac{\psi_{dr}\frac{\mathrm{d}}{\mathrm{d}t}\psi_{dr} + \psi_{qr}\frac{\mathrm{d}}{\mathrm{d}t}\psi_{qr}}{\psi_{dr}^2 + \psi_{qr}^2 - L_m\left(\psi_{dr}i_{ds} + \psi_{qr}i_{qs}\right)}. \tag{9}$$

Under these conditions, on the basis of the variables estimated by the Extended Luenberger Observer (ELO), rotor time constant can be estimated as so:

$$\frac{1}{\hat{T}_r} = -\frac{\hat{\psi}_{dr}\frac{\mathrm{d}}{\mathrm{d}t}\hat{\psi}_{dr} + \hat{\psi}_{qr}\frac{\mathrm{d}}{\mathrm{d}t}\hat{\psi}_{qr}}{\hat{\psi}_{dr}^2 + \hat{\psi}_{qr}^2 - L_m^*\left(\hat{\psi}_{dr}\hat{i}_{ds} + \hat{\psi}_{qr}\hat{i}_{qs}\right)}. \tag{10}$$

Under these conditions, the coefficients of the ELO, which are calculated according to the estimated stator and rotor time constants, are:

$$a_{11}^* = -\left(\frac{1}{\hat{T}_s}\cdot\frac{1}{\sigma^*} + \frac{1}{\hat{T}_r}\cdot\frac{1-\sigma^*}{\sigma^*}\right);\ a_{13}^* = \frac{1}{\hat{T}_r}\cdot\frac{L_m^*}{L_s^*L_r^*\sigma^*};\ a_{31}^* = \frac{L_m^*}{\hat{T}_r};\ a_{33}^* = -\frac{1}{\hat{T}_r}. \tag{11}$$

The block diagram of the extended Luenberger observer (ELO), adapted to the stator and rotor time constants, is shown in Fig. 2.

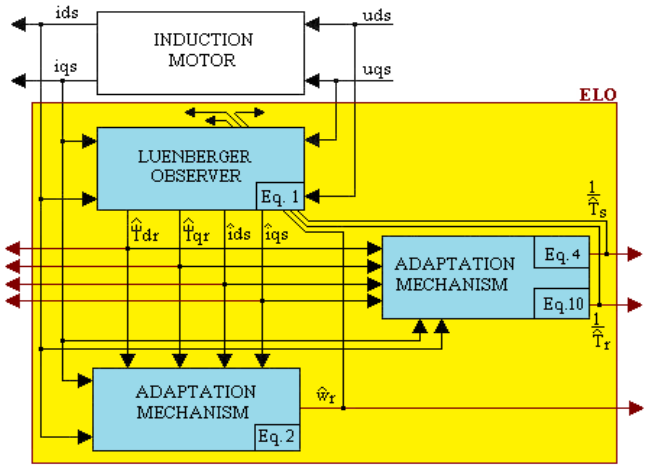

Fig. 2 − The Extended Luenberger Observer – with compensation.

In order to cancel the zero division, which occurs periodically within (10), due to the cancellation of the denominator, we will use the Fixed Trace method. In this regard, we will use the following notations:

$$X = -\left(\hat{\psi}_{dr} \frac{\mathrm{d}}{\mathrm{d}t} \hat{\psi}_{dr} + \hat{\psi}_{qr} \frac{\mathrm{d}}{\mathrm{d}t} \hat{\psi}_{qr} \right), \tag{12}$$

$$Y = \hat{\psi}_{dr}^2 + \hat{\psi}_{qr}^2 - L_m^* \left(\hat{\psi}_{dr} \hat{i}_{ds} + \hat{\psi}_{qr} \hat{i}_{qs} \right). \tag{13}$$

Under these conditions, the inverse of the rotor time constant, estimated using the Fixed Trace method, is (Pana *et al*., 1995), (Pana, 1996)

$$\hat{\theta}(nT_e) = \hat{\theta}\left[(n-1)T_e\right] - K\left[nT_e\right] E\left[nT_e\right]; \quad n = 0,1,2,\ldots \tag{14}$$

where:

$$K\left[nT_e\right] = \frac{\gamma Y\left[nT_e\right]}{1+\gamma\left(Y\left[nT_e\right]\right)^2}; \; \hat{\theta}(nT_e) = \frac{1}{\hat{T}_r(nT_e)}; \; \left.\hat{\theta}\right|_{n=0} = \frac{1}{T_r^*};$$
$$E\left[nT_e\right] = Y\left[nT_e\right]\hat{\theta}\left[(n-1)T_e\right] - X\left[nT_e\right].$$

Within the relation (14) T_e is the sampling time and γ is forgetting factor ($\gamma > 0$). In order to determine the rotor time constant, the relation (12) is discretized by the Euler method. Relationships (12) and (13) in discrete-time, are

$$X(nT_e) = -\left[\hat{\psi}_{dr}(nT_e)\Delta_{dr}(nT_e) + \hat{\psi}_{qr}(nT_e)\Delta_{qr}(nT_e)\right], \tag{15}$$

$$Y(nT_e) = \hat{\psi}_{dr}^2(nT_e) + \hat{\psi}_{qr}^2(nT_e) - L_m^* \alpha(nT_e), \tag{16}$$

where:

$$\Delta_{dr}(nT_e) = \frac{\hat{\psi}_{dr}(nT_e) - \hat{\psi}_{dr}\left[(n-1)T_e\right]}{T_e} \tag{17}$$

$$\Delta_{qr}(nT_e) = \frac{\hat{\psi}_{qr}(nT_e) - \hat{\psi}_{qr}\left[(n-1)T_e\right]}{T_e} \tag{18}$$

$$\alpha(nT_e) = \hat{\psi}_{dr}(nT_e)\hat{i}_{ds}(nT_e) + \hat{\psi}_{qr}(nT_e)\hat{i}_{qs}(nT_e). \tag{19}$$

4. The Vectorial Control System

The extended Luenberger observer (ELO) is tested by simulation in Matlab-Simulink within the sensorless vector control system, shown in Fig. 3.

The control system of Fig. 3 is one with direct orientation after rotor field (DRFOC).

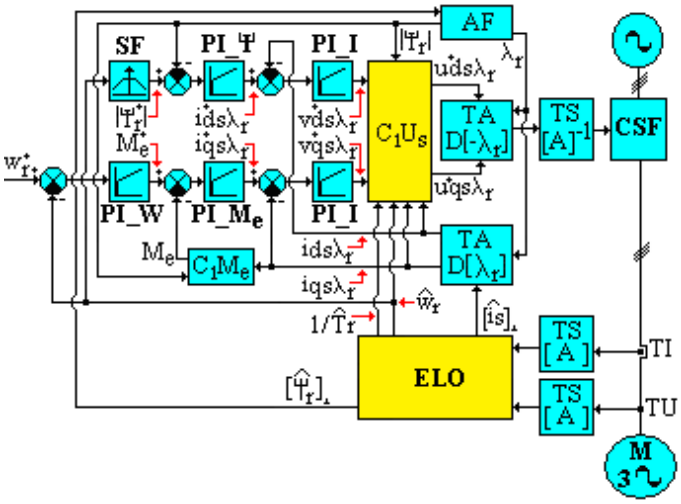

Fig. 3 − The block diagram of the vector control system.

The main blocks within the vector control system are defined by the following equations (Pană, 2016):

- stator voltages decoupling block (C_1U_s)

$$\begin{cases} u^*_{ds\lambda_r} = \dfrac{1}{b^*_{11}}\left[b^*_{11}v^*_{ds\lambda_r} - h_1\right] \\ u^*_{qs\lambda_r} = \dfrac{1}{b^*_{11}}\left[b^*_{11}v^*_{qs\lambda_r} + h_2\right] \end{cases} \tag{20}$$

where:

$$h_1 = a^*_{13}\left|\hat{\psi}_r\right| + a^*_{31}\frac{\hat{i}^2_{qs\lambda_r}}{\left|\hat{\psi}_r\right|} + z_p\hat{\omega}_r\hat{i}_{qs\lambda_r}\ ;\ \left|\hat{\psi}_r\right| = \sqrt{\hat{\psi}^2_{dr} + \hat{\psi}^2_{qr}}\ , \tag{21}$$

$$h_2 = a^*_{14}z_p\hat{\omega}_r\left|\hat{\psi}_r\right| + a^*_{31}\frac{\hat{i}_{ds\lambda_r}\hat{i}_{qs\lambda_r}}{\left|\hat{\psi}_r\right|} + z_p\hat{\omega}_r\hat{i}_{ds\lambda_r}\ . \tag{22}$$

The coefficients within relations (20),…,(22) are identical to those in the extended Luenberger observer (ELO).

The C_1U_s block is adjusted in according to speed and the rotor time constant.

- the field weakening block (SF)

$$\left|\psi_r^*\right| = \begin{cases} \dfrac{U_{\max} g}{2\pi f_N} & \text{if} \quad \left|\hat{\omega}_r\right| \le \dfrac{2\pi n_N}{60} \\ \dfrac{L_m^*}{R_s^*} \cdot \dfrac{g U_N \sqrt{\dfrac{2}{3}}}{\sqrt{1 + z_p^2 \left(T_r^*\right)^2 \hat{\omega}_r^2}} & \text{otherwise} \end{cases} \tag{23}$$

where: $g = 1 + A_m \left[\sin\left(\omega_1 t\right) + \sin\left(\omega_2 t\right)\right]$; $\omega_1 = 2\pi f_1$; $\omega_2 = 2\pi f_2$.

In the relation (23), by U_N the rated voltage; f_N is rated frequency; n_N is the rated speed, of the induction motor. The five automatic controllers of the control system presented in Fig. 3, are Proportional Integral-type (PI). The other blocks of Fig. 3, are: current transducers (TI); voltage transducers (TU); static frequency converter (CSF); blocks of transformation of the system (TS) and axis (TA), flux analyzer (AF) and calculus of the torque block (C_1M_e).

5. Simulation results and discussion

The ELO observer is validated by simulation, using a 4 [kW] induction motor. The electro-mechanical parameters of the induction motor are presented in Table 1.

Table 1
Induction Motor Parameters

Symbol	Name	Value
R_s	Stator resistance	1.405 [Ω]
R_r	Rotor resistance	1.395 [Ω]
L_s	Stator inductance	0.178039 [H]
L_r	Rotor inductance	0.178039 [H]
L_m	Mutual inductance	0.1722 [H]
J	Motor inertia	0.0131[kg·m^2]
F	Friction coefficient	0.002985[N·m·s/rad]
n_N	Rated speed	1430 [rpm]
z_p	Number of pole pairs	2
U_N	Rated voltage	400 [V]
M_N	Rated torque	27 [N·m]
f_N	Rated frequency	50 [Hz]

The rest of the constants used within the simulation are presented in Table 2.

Table 2
Simulation Parameters

Symbol	Name	Value	Obs.
K_{RF}	Parameter of proportionality	370.5764	The rotor flux controller
K_{IF}	Parameter of integration	2903.6	
K_{RM}	Parameter of proportionality	0.1105	The torque controller
K_{IM}	Parameter of integration	110.5032	
K_{RW}	Parameter of proportionality	2.1833	The speed controller
K_{IW}	Parameter of integration	182.3178	
K_{RI}	Parameter of proportionality	11.4865	The current controllers
K_{II}	Parameter of integration	2710	
K_{Ra}	Parameter of proportionality	5.4943	Adaptation mechanism of the speed
K_{Ia}	Parameter of integration	43049.67	
K_{Rb}	Parameter of proportionality	0.01	Adaptation mechanism of the stator time constant
K_{Ib}	Parameter of integration	50	
T_e	The sampling time	1 [μ sec]	The estimator of the rotor time constant
γ	The forgetting factor	0.0008	
k	Parameter of proportionality	1.2	The proportionality coefficient of the ELO
f_1	Frequency	9 [Hz]	The frequency f_1 used in the SF block
f_2	Frequency	11 [Hz]	The frequency f_2 used in the SF block
A_m	Amplitude	0.02	The amplitude of the signal used in the SF block

From the Table 2, it is noticeable that the current controllers are identical. The transistors within the static frequency convertor with intermediary continuous voltage circuit are considered of ideal commutation.

Within simulation, the CSF disregards the mathematical models of the semiconducting devices. Within the PWM modulation, the carrier is of isosceles triangle type having a frequency of 5 [kHz]. The modulation technique is based on a modified suboscillation method (Holtz, 1994).

In simulation test, the induction motor is functioning under load, having at its ax a resistant torque equal to that of the rated torque of the induction motor. The vector control system shown in Fig. 3 is tested taking into account that the speed imposed on the control system is has two- step speed trapezoidal profile. The rise time from one speed step to another is 0.2 seconds, in the case of the speed imposed.

All tests are made assuming that the induction motor is preheated. As such, in the initial moment, the rotor resistance is considered with 20% higher than the rated value, while the stator resistance is considered with 15% higher than the rated value. After 5 seconds, the values for rotor and stator resistances are abruptly increased by 25% and 20% from their rated values.

The simulation program is shown in Fig. 4.

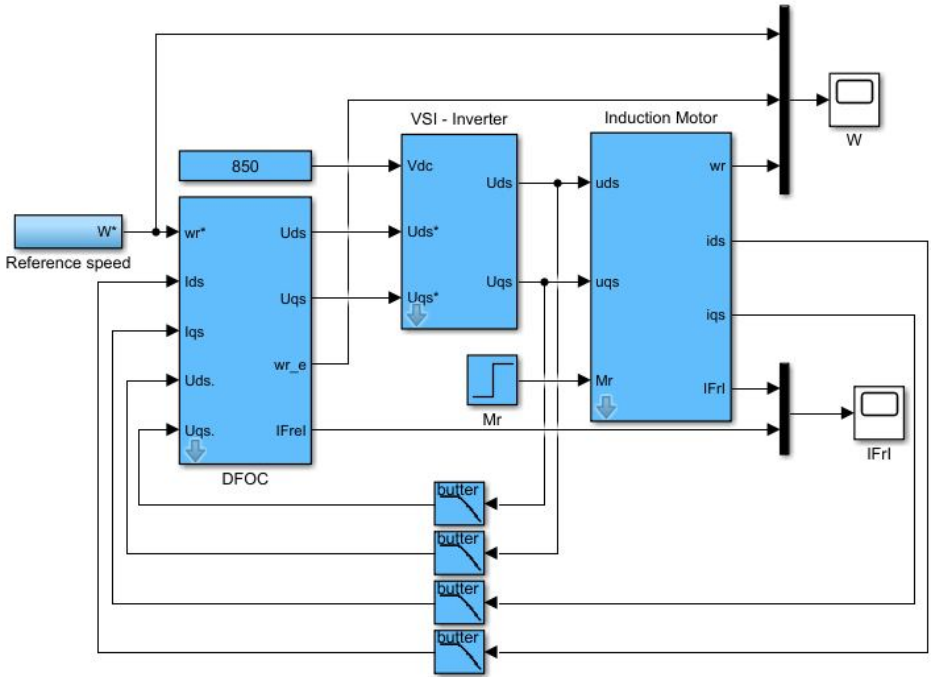

Fig. 4 − The simulation program of the sensorless vector control system.

In the simulation, stator currents and stator voltages, from the CSF output used in the extended Luenberger observer are filtered by means of second-order Butterworth low-pass filters, all of which have a cutting frequency of 500 [Hz].

At the initial moment of the simulation, the estimation block of the rotor time constant is not used. For 0.02 second, the rotor time constant is considered to have a value of

$$\frac{1}{\hat{T}_r(t)} = \frac{R_r^*}{L_r^*} \quad \text{if} \quad t \in [0 \quad 0.02][\text{sec}] \tag{24}$$

and then the block of the rotor time constant estimate is coupled.

In order to solve the differential equations defining the sensorless vector control system, was used Dormand – Prince method (ode 45), using both an relative and absolute error of the $\varepsilon = 10^{-6}$. The simulation time is 8 seconds.

The obtained results are presented in the following figures.

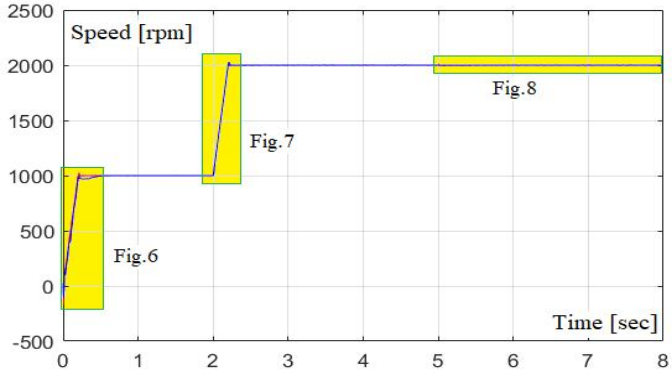

Fig. 5 – Time variation of imposed speed in tandem with measured speed and estimated speed of the induction motor.

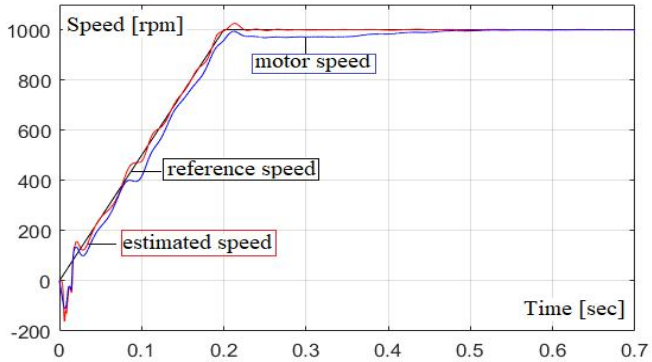

Fig. 6 – Highlighting the dynamic performance of the vector control system with respect to the time variation of the speed at the start of the induction motor.

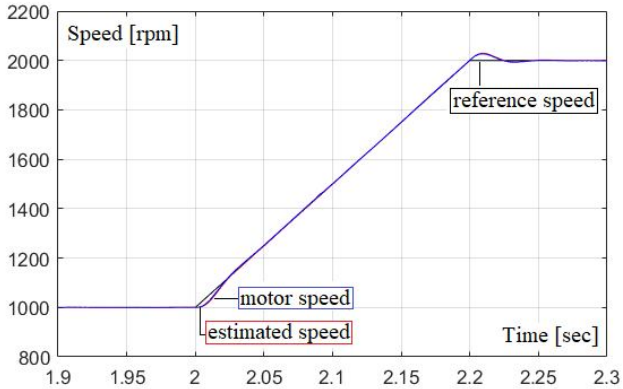

Fig. 7 – Highlighting the dynamic performance of the vector control system with respect to the time variation of the speed, at the when passing from step 1 to step 2 of the speed.

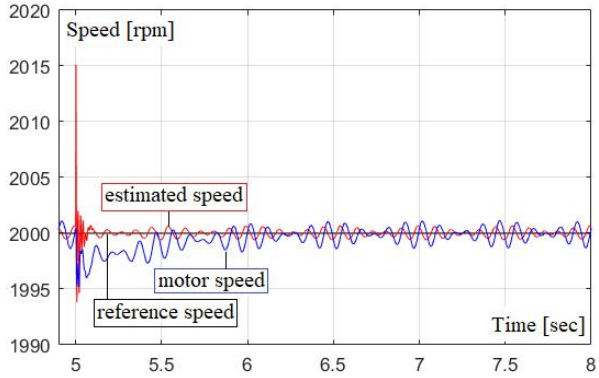

Fig. 8 – Evidence of the dynamic performance of the vector control system regarding the time variation of the speed, immediately after the sudden variation of the rotor resistance and stator resistance in stationary regime.

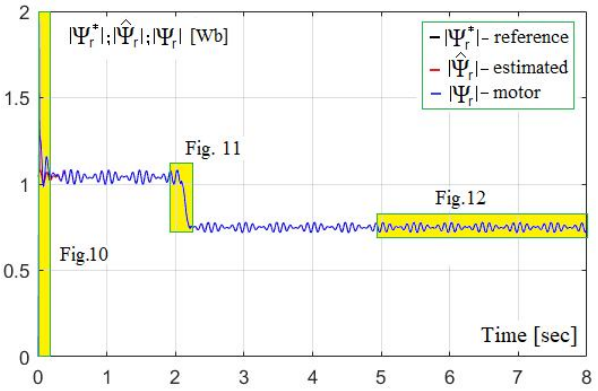

Fig. 9 – The variation in time of the imposed phasor of the rotor flux, in tandem with the real and estimated rotor flux phasor of the induction motor.

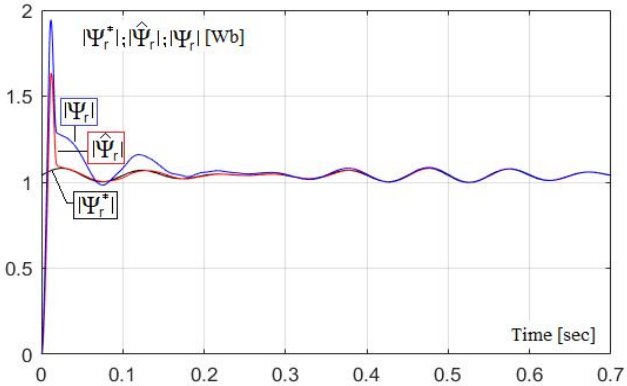

Fig. 10 – Highlighting the dynamic performance of the vector control system with respect to the time variation of the phasor of the rotor flux, when starting the induction motor.

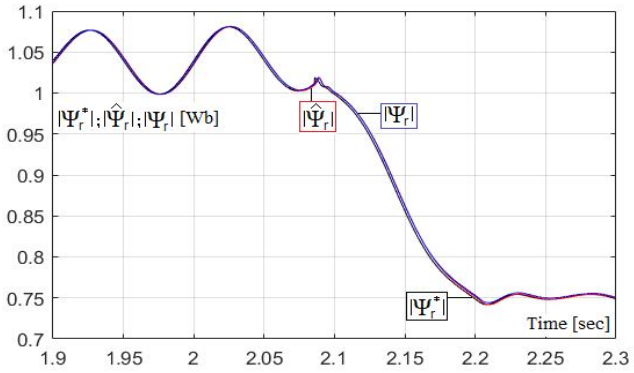

Fig. 11 – Highlighting the dynamic performance of the vector control system with respect to the time variation of the rotor flux phasor, at the when passing from step 1 to step 2 of the trapezoid speed profile.

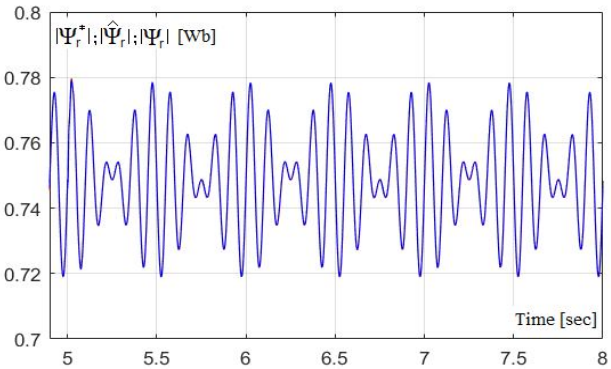

Fig. 12 – Evidence of the dynamic performance of the vector control system regarding the time variation of the rotor flux phasor, immediately after the sudden variation of the stator resistance and rotor resistance in stationary regime.

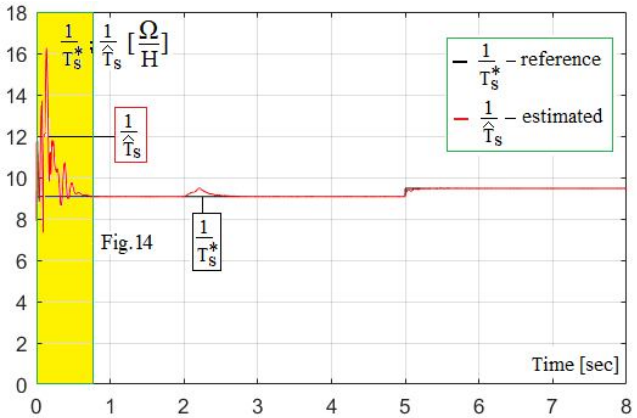

Fig. 13 – The variation in time of the stator-time constants - of the reference and estimated.

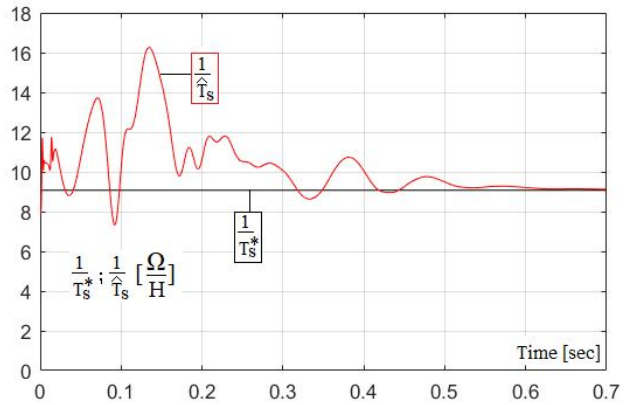

Fig. 14 – Highlighting the dynamic performance of the vector control system with regard to the time variation of the stator-time constant, at the start of the induction motor.

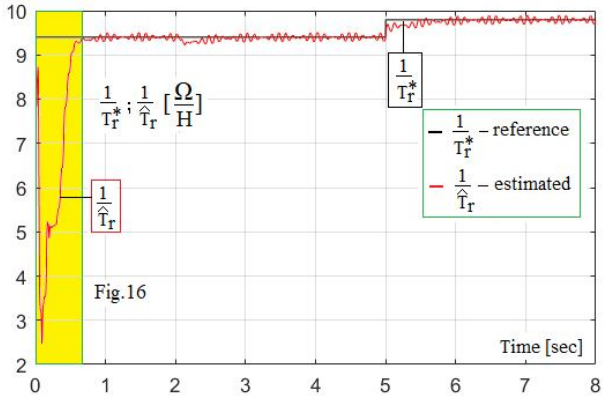

Fig. 15 – The variation in time of the rotor – time constants – of the reference and estimated.

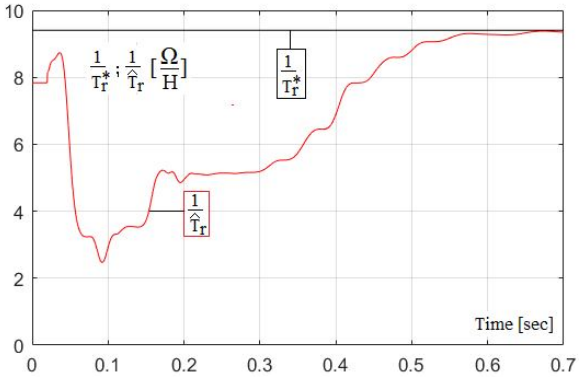

Fig. 16 – Highlighting the dynamic performance of the vector control system with regard to the time variation of the rotor – time constant, at the start of the induction motor.

From the previously presented graphs we can see that the vector control system in Fig. 3, has very good dynamic performances.

On the other hand, it can be seen from Figs. 13 and 15 that the estimation of the rotor and stator time constants are affected by the speed variation over time (these are observed when starting the induction motor and at the time of t = 2 second). This effect is canceled after about 0.7 second (see Figs. 13,…,16). The maximum deviation from the reference value is 7.185 [Ω/H], in the case of the estimation of the stator time constant, and 6.932 [Ω/H] in the case of estimation of the rotor constant of the induction motor.

When the rotor resistance and stator resistance increases by 25% and 20% respectively, compared to their rated value (see t = 5 second), it can be seen that the rotor time constant is estimated correctly after approximately 1 second (see Fig. 15), respectively 0.4 second in case of estimation stator time constant (see Fig. 13). When the rotor time and stator time constants is estimated correctly, the reference speed overlaps with the estimated speed and the measured speed of the induction motor (this is observed in Figs. 6 and 8).

From Fig. 9 shows that when the reference speed pass in from step 1 to step 2, by means of the *SF* block within the vector control system, a rotor flux is reduced (weakening). From Figs. 9,…,12 it can be seen that the extended Luenberger observer (ELO) very well estimates the modulus of the rotor flux phasor. When starting the induction motor, the phasor of the measured rotor flux overlaps with the phasor of the estimated rotor flux and with reference, after approximately 0.2 seconds (Fig.10).

6. Conclusions

The compensation solution of the extended Luenberger observer (ELO), described in this article, has the following advantages:

- the estimator has a very good convergence, with the settling time being less than 1 second, in the case of a sudden change in rotor resistance, respectively 0.4 second, in the case of a sudden change in stator resistance;
- reduces errors in estimating speed and rotor flux in the case of variation in time of rotor and stator resistance, so that the dynamic performances of the sensorless vector control systems is much better;
- the parametric stability domain of the sensorless vector control system is much greater than if the extended Luenberger observer is not compensate (Pană, 2010);
- the use of a sensorless vector control system containing an extended Luenberger observer (ELO) compensated by the rotor and stator time constants, allows the elimination of auxiliary ventilation systems of the induction motors.

Given the above, we consider that the proposed method of the extended Luenberger observer (ELO) compensation can be successfully used within industrial applications.

REFERENCES

Holtz J., *Pulsewidth Modulation for Electronic Power Conversion*, Proc. of IEEE, **82(8)**, 1194-1214 (1994).

Kubota H., Matsuse K., *DSP-Based Speed Adaptive Flux Observer of Induction Motor*, IEEE Tans. Ind. Appl., **29(2)**, 344-348 (1993).

Kubota H., Matsuse K., *Speed Sensorless Field-Oriented Control of Induction Motor with Rotor Resistance Adaptation*, IEEE Tans. Ind. Appl., **30(5)**, 1219-1224 (1994).

Pană T., Hori Y., *Simultaneous Speed Estimation and Rotor Resistance Identification for Sensorless Induction Motor Drives*, Proc. of IPEC, 1995, Yokohama, Japan, 316-321.

Pană T., *Model Based Speed and Rotor Resistance Estimation for Sensorless Vector-controlled Induction Motor Drives using Floating Point DSP*, 1996, Proc. of AMC, Mie, Japan, **1**, 168-173.

Pană T., Stoicuță O., *Design of an Extended Luenberger Observer for Sensorless Vector Control of Induction Machines under Regenerating Mode*, Proc. of IEEE Conf. OPTIM, 2010, Braşov, România, 469-478.

Pană T., Stoicuță O., *Stability of the Vector Drive Systems with Induction Motors*, Mediamira Publishers, Cluj –Napoca, România, 2016.

Shinnaka S., *A Unified Analysis on Simultaneous Identification of Velocity and Rotor Resistance of Induction Motors*, Trans. Institute of Electrical Engineers of Japan, **113-D(2)**, 1483-1484 (1993).

COMPENSAREA ONLINE A EFECTELOR CAUZATE DE VARIAȚIILE PARAMETRILOR ELECTRICI AI MOTORULUI DE INDUCȚIE PENTRU ESTIMATORUL LUENBERGER EXTINS

(Rezumat)

Articolul prezintă o soluție de compensare a efectelor cauzate de variațiile parametrilor electrici ai motorului de inducție pentru estimatorul Luenberger extins (ELO), utilizat în estimarea simultană a vitezei, poziției şi a modulului fazorului fluxului rotoric. ELO este ajustat în funcție de constantele de timp estimate ale statorului si ale rotorului. Constanta de timp a rotorului este estimată pe baza unei relații deduse din modelul matematic al motorului de inducție. Performanțele dinamice ale estimatorului Luenberger extins sunt evidențiate prin simulare în Matlab – Simulink.